Available online at www.sciencedirect.com
ScienceDirect
Procedia Engineering 2 (2010) 639–647
Procedia Engineering
www.elsevier.com/locate/procedia

Fatigue 2010

Effect of cold driving process on fatigue life of helicopter fuselage joints

Fabio Viganò[a], Andrea Manes[a]*, Marco Giglio[a]

[a]*Politecnico di Milano, Dipartimento di Meccanica, Via la Masa 1, Milano, 20156, Italy*

Received 1 March 2010; revised 9 March 2010; accepted 15 March 2010

Abstract

Cold driving is a common procedure in aeronautical structures in presence of riveted holes; this process has influence on the fatigue life of the whole riveted joint. Using detailed FE models comprehensive of the rivet forming operation, the effect of the squeeze force on fatigue life of the joint has been investigated. Different multiaxial fatigue criteria (Sines, Crossland, Kakuno-Kavada and Papadopoulos) have been used in the fatigue evaluations in order to consider the complete stress state of the riveted hole (comprehensive of the residual stress field). The numerical analyses have been supported by an experimental test carried out on a panel specimen from rotorcraft frame.

Keywords: Revited joint, Finite element, Fatigue, Rotorcraft

1. Introduction

Rotorcraft frames are complex structures that are composed by many subassemblies joined together. From a structural point of view, these structures must be assessed for how concern fatigue loads. The European Certification Specification CS 29.571 [1] drives the manufactures on the fatigue criteria and conditions that the components must satisfy. Safe-life, Enhanced Safe-life, Damage Tolerant and Fail-safe are all methods used by the designer and chosen in base of the component criticality. Riveted joints are a present issue in rotorcraft structures because they transmit the flight loads between the components. Rivets are commonly used in the metallic joint due to their low cost and low assembly time. The drawback of the rivets is focused on their limited strength and their effects on the joint due to the riveting process. In fact, the riveting forming quality can be inflected by the technicians' experience. Commonly, the riveting operations have been done by technicians using a pneumatic or a hydraulic riveting gun that can control only the maximum squeeze force (maximum force during the rivet forming).
The squeeze force is a parameter which influenced the fatigue life of the joint; in fact, difference in the squeeze force induces different deformations on the rivet, and consequentially, different residual stress on the riveted holes. The riveted joint design criteria are usually based on the maximum static strength allowable on the rivets and on the hole (bearing loads). The detailed procedure is reported in the military handbook MIL -HDBK-5J [2]. From a fatigue point of view, at paragraph 571, CS-29 [1] suggests that riveted joint should be designed using classical

* Corresponding author. Tel.: +39 0223998630; fax: +39 0223998282.
E-mail address: andrea.manes@polimi.it

1877-7058
doi:10.1016/j.proeng.2010.03.069

Safe-Life methodology; notwithstanding the joints on which they are used, can be designed using Fail-Safe or in general a Damage-Tolerance approach [3]. Effectively, the major failures of a joint are related to fatigue cracks that nucleate in the rivet holes and propagate until they reach the slant fracture.
The riveted joint analyzed in this work is featured by a complex geometry, contacts, interference between rivet shank and holes and residual stresses; considering all these factors a detailed 3D finite element model is fundamental for a reliable fatigue evaluations. As already introduced, a parameter that has a significant impact on a riveted joint is the squeeze force. This force determine the geometry of the deformed rivet, the expansion and consequentially also the stress field on the hole. According to the actual "state of the art" this is the major factor that characterizes the fatigue life of the joint. Urban [4] point out this influence and reports also a complete literature review about the parameters (interference, rivet length, etc.) that have influence on the riveted joint integrity. Differently, Müller [5] carried out an extensive experimental program that shows clearly the influence of the squeeze force on the fatigue life of the joint. Rijck et al. [6] conduct a study in which they consider the driven rivet head dimensions as indication of the fatigue performance of the joints. The residual stresses are studied by Rans et al. [7] using a 3D FE simulation that reproduces the riveting operations. A simplified study of the residual clamping stress has been also done by Deng and Hutchinson [8]; they investigate the stresses using a 2D simplified FE model of the riveting and extrapolating simply equations for its estimation.
Szolwinski et al. [9] confirm experimentally the importance of the residual stress state on the fatigue life. Together the residual stress field, an hole expansion is generated during the riveting procedure. These effects are similar to the ones produced by the so called "cold-expanded" hole operations. In particular application, the riveted holes are expressly cold expanded with the object to improve the fatigue life of the riveted joint.
The residual stresses induced by this method are more higher and controllable than the residual stress induced only during the riveting procedure; the residual stresses of the cold expansion and they effect on the crack propagation have been studied in detail by P.F.P. de Matos et al. [10][11].
In this paper, the fatigue life of a riveted joint have been analyzed on a panel representative of the real one from an helicopter frame. The panel in Figure 1a has been built up like a common aircraft structure; it is composed by stringers, skin, T-cleats and rivets. The panel has also been tested experimentally in a dedicated frame by an harmonic fatigue cycle. The part under test has been the so-called "rear modular joint" that is joint in the lower constraint part of the panel. In particular the T-cleats is the most critical component due to the fact the constraints forces pass directly trough this part. In the Figure 1b the fatigue failure in the T-cleat hole at rivet interface is clearly visible. T-cleats and stringers have been made of Al8090-T81; all the others components have been made of Al 2024. The aluminium alloys are materials commonly used in aircraft structures due to their lightness and good mechanical strength; in particular, the aluminium alloy Al 8090 is well known due to its extreme lightness thanks to the presence of Lithium. Moreover it has a Young modulus of 11% greater than the common aluminium alloy and these features confer it very interesting design properties. The mechanical properties of the materials used in this work are reported in Table 1.

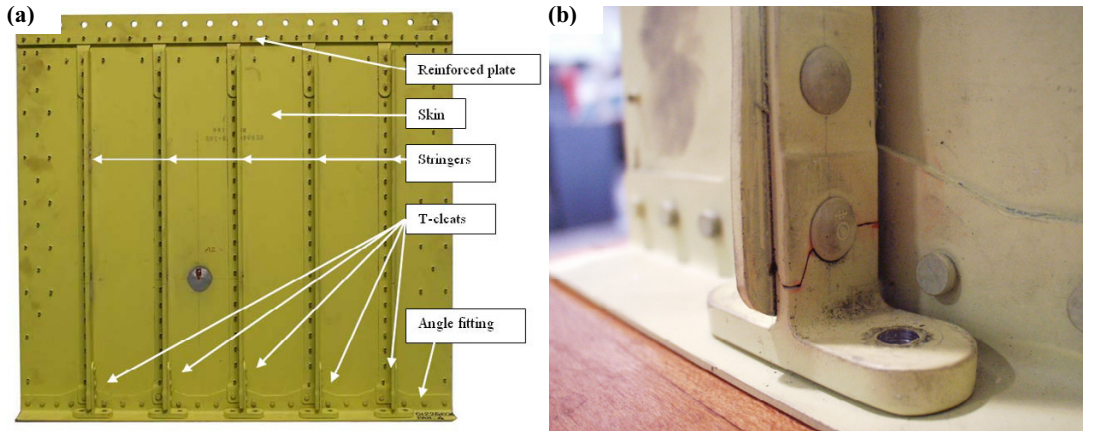

Fig. 1. (a) Helicopter's panel under analysis; (b) The lower part of the panel is the real modular joint under test. It is clearly visible a crack in the lower rivet of the T-cleat

The residual stresses and the effect of the squeeze force variation (i.e. hole expansion) on the joint structural integrity have been investigate using a detailed 3D finite element model with sub-modelling technique. A global 3D FE model represent the complete panel specimen, and a first sub-model reproduce in detail the features of the joint and the last sub-model reproduce the riveting forming operation.
Thanks to this powerful tool of virtual simulations, it has been possible to change the riveting parameter related to the squeeze force and to analyze their effects. A work focused on a similar approach has been done by Cheraghi et al. [12] with particular attention on the riveting quality.

Table 1. Material characteristics

Material	E [MPa]	υ	σ_Y [MPa]	S_u [MPa]	ε_f	*K [MPa] - n*
Al 2024 [13]	73100	0.33	317	330	-	338.5 - 0.01
Al 8090-T81 [14]	77000	0.30	324	450	0.12	-

2. Finite element models

Three finite element models have been used in this work in order to model efficiently all the aspects of the riveted joint. At first, a general Panel FE model (Figure 2) including all the components of the panel in the test configuration has been carried out. Skin, stringers, angle fitting, reinforcement have been modeled with shell elements. The T-cleats are instead reproduced using solid elements (C3D8R). All the rivets and bolts have been reproduced by beam elements connected by kinematics constrains to the holes. Between all the components a contact interaction has been imposed with a friction coefficient of 0.19. The T-cleats have been bolted to the ground and a force has been applied at the top of the panel. The joint FE model is a sub-model that reproduces in detail the joint geometry using a total of 65000 3D finite elements. These two models have been built-up in Abaqus/Standard v6.7 with linear elastic material properties. Finally, the riveting FE sub-model has been realized to simulate the complete process of riveting forming.

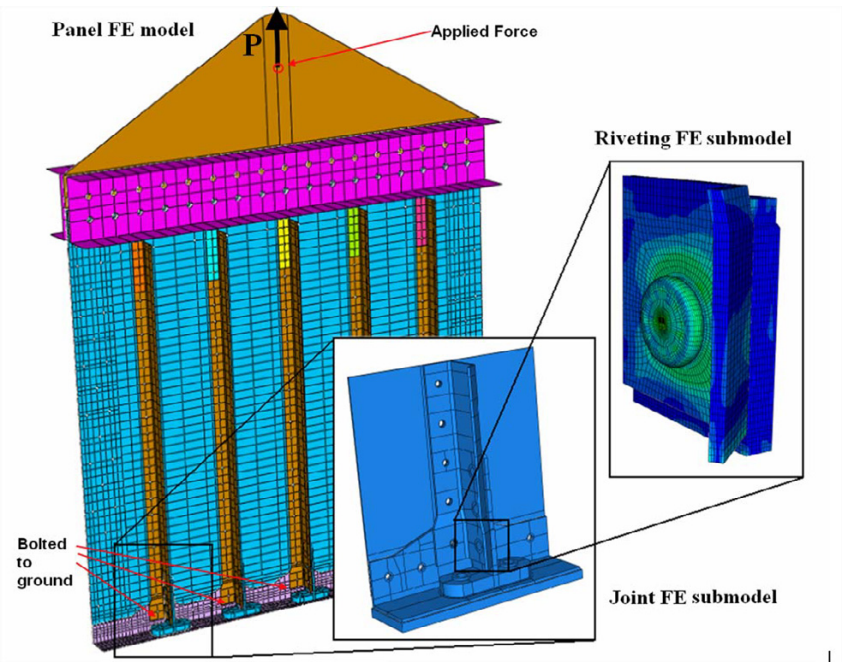

Fig. 2. FE models

This last simulation has been affected by high non-linearity (material plasticity, contacts, high deformations) and in order to solve them, a explicit solver have been used (Abaqus/Explicit v6.7). The solid rivet made of Al 2024 [13] has been modeled as elastic-plastic material with linear hardening behavior (from yield point to failure condition). The stringer and the T-cleat have been both modeled in a similar way, considering the application of Al 8090-T81 material data (Table 1), [14].
Figure 3a shows the characteristic dimensions of the rivet before and after the rivet forming. The riveting simulation has been done by a rigid surface (Figure 3b) which compress the rivet head until it reached the measured dimension of the deformed rivet on the specimen panel (Figure 4). Excessive mesh distortions have been avoided applying the Arbitrary Lagrangian - Eulerian (ALE) [15] technique on the rivet domain.

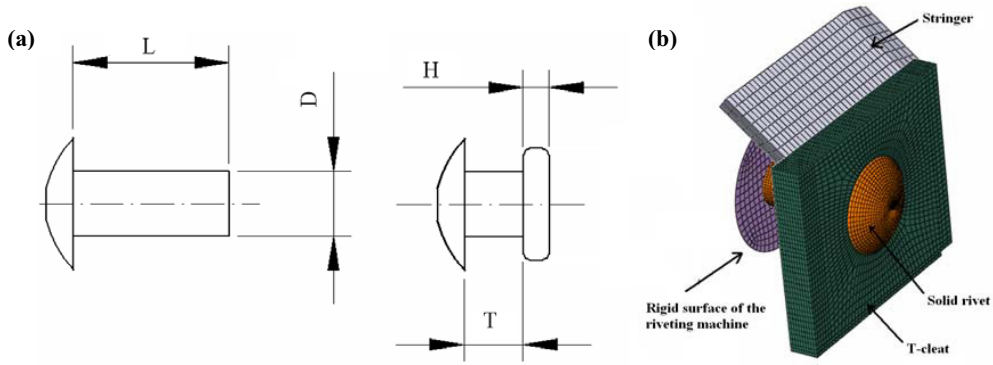

Fig. 3. (a) Rivet geometry before and after the deformations; (b) FE Riveting sub-model.

L is the length and *D* is the diameter of the rivet shank before riveting. *T* is the dimension of the sheets to join and *H* is the upset head height. In the configuration used in the experimental tests, the rivet geometry is characterized by a diameter of 4.76mm (3/16 inch.), a length *L* equal to 11.1mm, a total sheets thickness (*T*) of 4.3mm and a upset height *H* equal to 2.0mm. This configuration respects the rule of thumb (used by the designer) in which the rivet length *L* minus the total sheet thickness *T* should be about one time and half the rivet diameter *D* [16].

3. Experimental test

The panel in test configuration has been experimentally tested on a dedicated frame. The force P has been generated by a hydraulic actuators. The applied force P, Figure 2, varies harmonically from a maximum of 19600N to a minimum of 1960N (load ratio *R*=0.1). The failure happens on the T-cleat hole (Figure 1b) after 1,750,630 cycles.
Moreover, a series of strain measures have been used to validate the Panel FE model; the average error between the experimental and the numerical measures has been of about 10%.

4. Effects of the squeeze force variations

As already introduced, the squeeze force play an important role in riveted joint fatigue integrity. Using the simulations (virtual tests) it has been possible to quantify the stress distribution and its variation with the different parameters involved in the problem. Varying the squeeze force, the riveted hole expands and the residual stress field changes consequentially. Two output parameters have been processed to analyze the parameter variation effects:

- The highest first principal stress σ_I in the riveted hole (Figure 5). This stress is close to the circumferential stress $\sigma_{\vartheta\vartheta}$ and it is representative of the way in which the fatigue crack in the hole happens and propagates.

- The mean of the first principal stress $\hat{\sigma}_I$ (fig.5) along the T-cleat thickness on the generatrix that includes the most stressed points σ_I.

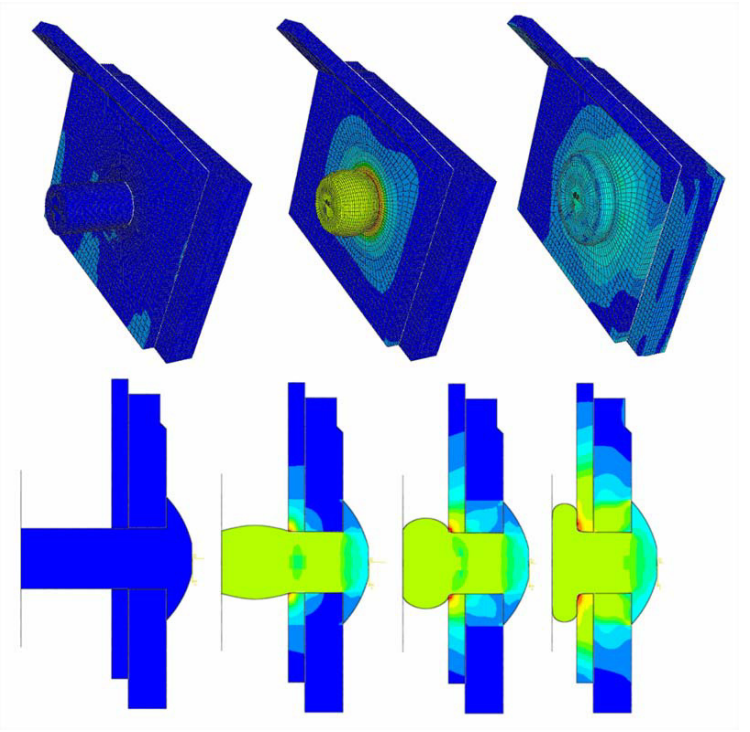

Fig. 4. The rivet forming result.

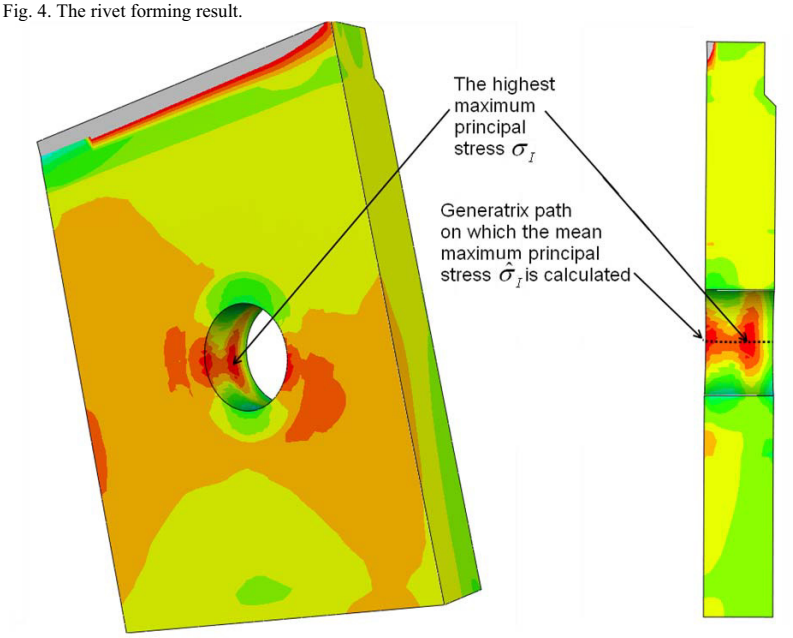

Fig. 5. The stress parameter taken into consideration in the analysis of the effects

In a riveting machine, the technician regulates the pressure valve in order to control the squeeze force until it obtains satisfied deformed rivet geometry. The Standard Aircraft Handbook [16] shows the dimension range of the upset height in which the riveting operations are assumed valid. For the analyzed rivet (4.76mm or 3/16inch of shank diameter), the upset height can vary from 1.98mm (1/8inch) to 3.18mm (5/64inch).
The squeeze force variations have been obtained in the FE simulations varying the motion of the rigid surface (Figure 3b) in order to obtain different rivet upset head height *H*.
Decreasing the upset height, the force requested increases; an analytical model (1) permits a prevision of the squeeze force. That model is based on the volume conservation of a mono-axial pressed bar [6]; D_f represents the final rivet head diameter, *K* - *n* are the material coefficients of the Ramberg-Osgood equation (Table 1), *L* - *H* are the rivet dimensions (Figure 3a) and *T* is the total thickness of the sheets to joint.

$$F_{sq} = \frac{1}{4} \cdot \pi \cdot D_f^{\,2} \cdot K \cdot \left(2 \cdot \ln\left(\frac{L-T}{H} \right) \right)^n \tag{1}$$

The results in Figure 6 show that analytical results underestimate the squeeze force respect to the FE results; that is a limitations of the analytical model which considers only the principal deformation variable and neglect the friction effects.

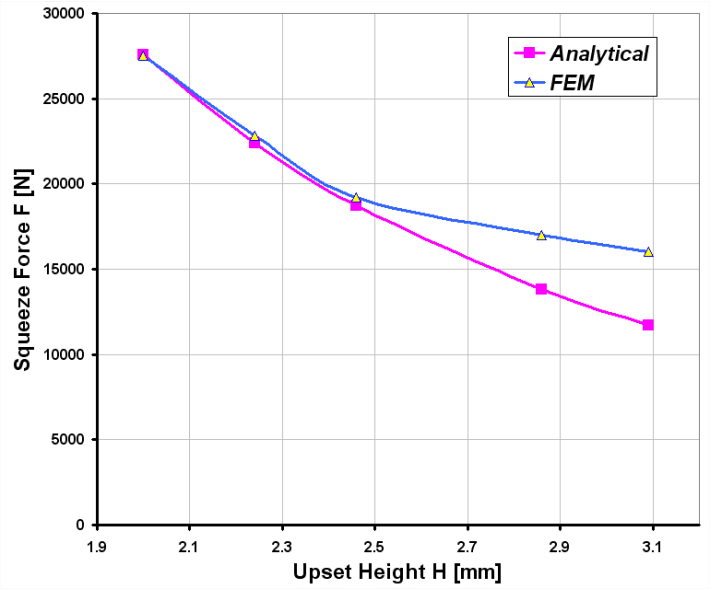

Fig. 6. The squeeze force versus the upset height

Figure 7a reports the trend of the maximum stress at the hole interface varying the squeeze load. The residual stress (that is the stress due only to the simulation of the riveting process) in the most stressed node has a high variability due to the fact that its position varies when a different squeeze force is applied. The "loaded "stress is the stress after the whole process: riveting and application of the load used in the experimental test (P_{max}=19.6kN with the load ratio *R*=0.1). The mean stress along the T-cleat thickness (Figure 7b) is a more representative parameter of what happens varying the squeeze force. When it increases, also the compressive residual stresses at unloaded condition increase and decrease the stresses on the hole in the loaded configuration.

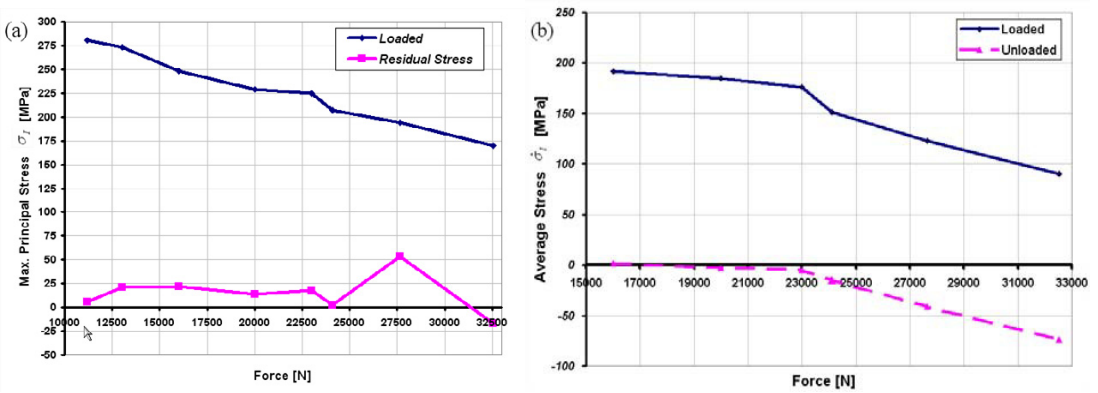

Fig. 7. (a) Punctual stress versus the Squeeze Force; (b) Average maximum stress versus Squeeze Force.

5. Fatigue evaluations

The stress field generated at hole interface has been post-processed by different multiaxial criteria in order to asses a fatigue predictions. As previous described, for unload conditions, the hole stress state has been characterized by the residual stress induced during the rivet forming. In the loaded panel configuration, the final stress field at hole has been composed by the residual stress added on the stress generated by the load. In both the configurations, the principal stresses are close to the normal stress ($\sigma_{rr}, \sigma_{\theta\theta}, \sigma_{zz}$) of a cylindrical reference system placed in the hole axis. Considering this approximation, the stress cycles can be considered proportional and in phase. That condition has permitted the use of a wide range of multiaxial criteria. Sines, Crossland, Kakuno-Kawada and Papadopoulos are the criteria used for fatigue evaluations with the fatigue data of Al8090-T81 reported by Birt and Beevers [14]. Elaborating these fatigue data, the relation (2) has been obtained.

$$\sigma_{F,R=-1}(N) = A \cdot (\log_{10}(N))^3 + B \cdot (\log_{10}(N))^2 + C \cdot \log_{10}(N) + D \tag{2}$$

The coefficients are *A=-7.065, B=138.64, C=-922.14* and *D=2153.6.* This expression has a correlation coefficient equal to R^2=0.99. Sines, Crossland and Kakuno-Kawada are all criteria based on stress invariants and they can be used for proportional stresses.

Sines is one of the oldest multiaxial fatigue criteria, it is easy to implement and generally give out conservative estimations [17]. Using this criterion, the failure cycles have been computed solving the relation (3). The term a_C has been considered equal to 1.53 and cycles independent. This value represents a mean of a_C coefficient referred to aluminum alloy and reported in the FatLim [18] database.

$$\sqrt{J_{2,a}} + \left(3 \cdot \frac{\tau_{R=-1}(N)}{\sigma_{a,R=0}(N)} - \sqrt{3} \right) \cdot \sigma_{H,m} = \tau_{R=-1}(N) \tag{3}$$

$$a_C = \frac{\sigma_{a,R=-1}(N)}{\tau_{R=-1}(N)} \tag{4}$$

The parameter $\sigma_{a,R=-1}$ is the axial fatigue limit with fully reversing cycle; $\tau_{R=-1}$ is instead the torsion fatigue limit with fully reversing cycles. $\sigma_{M,m}$ is the mean hydrostatic stress during the fatigue cycle and $\sqrt{J_{2,a}}$ is the second

invariant of deviator alternate stress tensor. The Crossland criterion (3) is similar to the Sines one but it consider the maximum hydrostatic stress $\sigma_{M,\max}$ instead of $\sigma_{M,m}$. This criterion generally gives more accurate predictions than Sines.

$$\sqrt{J_{2,a}} + \left(3 \cdot \frac{\tau_{R=-1}(N)}{\sigma_{a,R=-1}(N)} - \sqrt{3} \right) \cdot \sigma_{H,\max} = \tau_{R=-1}(N) \tag{3}$$

The Kakuno-Kawada (4) [19] separate the effects of the amplitude and mean value of the hydrostatic stress:

$$\sqrt{J_{2,a}} + \left(3 \cdot \frac{\tau_{R=-1}(N)}{\sigma_{a,R=-1}(N)} - \sqrt{3} \right) \cdot \sigma_{H,a} + \left(3 \cdot \frac{\tau_{R=-1}(N)}{\sigma_{a,R=0}(N)} - \sqrt{3} \right) \cdot \sigma_{H,m} = \tau_{R=-1}(N) \tag{4}$$

The Papadopoulos integral energetic criterion (5) [20] have been also used:

$$\sqrt{T_a^{\,2}} + \left(3 \cdot \frac{\tau_{R=-1}(N)}{\sigma_{a,R=-1}(N)} - \sqrt{3} \right) \cdot \sigma_{H,\max} = \tau_{R=-1}(N) \tag{5}$$

where the terms T_a represents the resolved shear stress amplitude; the details for its computation are in the reference [20].

In Table 2 the results obtained for the application of the different fatigue criteria are shown.

Table 2. Life estimation results

Upset Height	Sines	Crossland	Kakuno-Kavada	Papadopoulus	Mean	Experimental
H=2.1	*2.765.505*	*3.054.220*	*665.898*	*510.805*	*1.749.107*	*1.750.630*
H=2.6	*352.780*	*404.826*	*152.641*	*195.513*	*276.440*	-
H=3.1	*154.069*	*164.812*	*93.051*	*108.851*	*130.196*	-

Considering an upset height of 2.1 mm, Kakuno-Kavada and Papadopoulus multiaxial criteria predict the failure much earlier than the experimental result. Differently, Sines and Crossland criteria overestimate the joint life. Moreover, all the criteria are in agreement with the increase of the fatigue life when the upset height decrease (an increase of the squeeze force). The high variation of the cycle estimation is due to different stress state and by the high sensibility of the fatigue curve (2) at small stress variations; furthermore the fatigue curve in the finite life is affected by a data dispersion. Notwithstanding, the mean value of the fatigue life estimations is very close to the experimental failure; considering the complex stress scenario the results obtained is very encouraging.

6. Conclusions

Riveted joints are important components in aircraft structure and their fatigue life depends on different factors: squeeze force, interference, geometry, configuration, etc. The squeeze force is one of the more important factors and its influence has been analyzed numerically on a specimen panel. A global FE model, a FE sub-model of the joint and a complete 3D model of the rivet forming have been used in order to obtain a detailed stress state comprehensive of the residual stresses in the riveted holes. Thanks to the numerical models, the variations of the stresses on the most loaded riveted hole have been investigated. The stresses on the most loaded riveted hole have been successively post-processed using different multiaxial fatigue criteria (Sines, Crossland, Kakuno-Kavada and

Papadopoulos). All these criteria put in evidence the sensibility of the fatigue strength of the riveted joint respect to the squeeze force.

References

[1] CS-29. - Certification Specification for large rotorcraft, European Aviation Safety Agency, Nov. 2008.
[2] Department of Defense, MIL-HDBK-5J - Metallic materials and elements for aerospace vehicle structures. 2003.
[3] Biasini M, Mariani U, Oggioni F. EH101 – Main rotor head components evaluation of the damage tolerance capability – *22nd European Rotorcraft Forum*, 1996, Brighton, UK.
[4] Urban MR. Analysis of the fatigue life of riveted sheet metal helicopter airframe joints, *Int. J. of Fatigue* 2003:25, pp.1013-1026.
[5] Muller RPG. An experimental and analytical investigation on the fatigue behavior of fuselage riveted lap joints. PhD thesis, *Delft University of Technology*. 1995.
[6] de Rijck JJM, Homan JJ., Schijve J, Benedictus R. The driven rivet head dimensions as an indication of the fatigue performance of aircraft lap joints. *Int. J. of Fatigue* 2007:29, pp. 2208-2218.
[7] Rans C, Straznicky PV. Riveting process induced residual stresses around solid rivets in mechanical joints, *J. of Aircraft* 2007:44-1.
[8] Deng X, Hutchinson JW. The clamping stress in a cold-driven rivet. *Int. J. of Mech*. Sciences 1998:40-7, pp. 683-694.
[9] Szolwinski MP, Farris TN, Linking riveting process parameters to the fatigue performance of riveted aircraft structures, *J. of Aircraft* 2000:37-1, pp. 130-137.
[10] de Matos PFP, Moreira PMGP, Camanho PP, de Castro PMST. Numerical simulation of cold working of rivet holes, *Finite Elements in Analysis and Design* 2005:41-9-10, pp. 989-1007.
[11] de Matos PFP, McEvily AJ, Moreira PMGP, de Castro PMST. Analysis of the effect of cold-working of rivet holes on the fatigue life of an aluminium alloy, *Int. J. of Fatigue* 2007:29-3, pp. 575-586.
[12] Cheraghi SH, Krishnan K., Bajracharya B. Effect of variations in the riveting process on the quality of riveted joints, *The Int. J. of Adv. Manufacturing Tech.* 2008:39-11-12, pp. 1144-1155.
[13] ASM International, ASM Handbook Volume 19, *Fatigue and Fracture*; 2000.
[14] Birt MJ, Beevers CJ, The fatigue response of the Aluminium-Lithium alloy, 8090, *Proceedings of the Fifth International Aluminium-Lithium Conference* Williamsburg, Virginia, pp.983-1037; 1989.
[15] SIMULIA - Abaqus Analysis User's Manual Version 6.7 - 2007.
[16] Reithmaier. Standard Aircraft Handbook for Mechanics and Technicians, 6th Edition, McGraw-Hill; 1999.
[17] Papuga J. Mapping of Fatigue Damages - Program Shell of FE-Calculation, PhD Thesis, CTU in Prague; 2005.
[18] FatLim database, 2007, http://www.pragtic.com.
[19] Papadopoulos IV, Davoli PP, Gorla C, Filippini M, Bernasconi A. A comparative study of multiaxial high-cycle fatigue criteria for metals - *Int. J. of Fatigue* 1997:19-3, pp.219-235.
[20] Papadopoulos IV. Fatigue limit of metals under multiaxial stress conditions: the microscopic approach. Technical note no. 1.93.10 1, ISEI/IE 2495/93. Commission of the European Communities, *Joint Research Centre*; 1993.